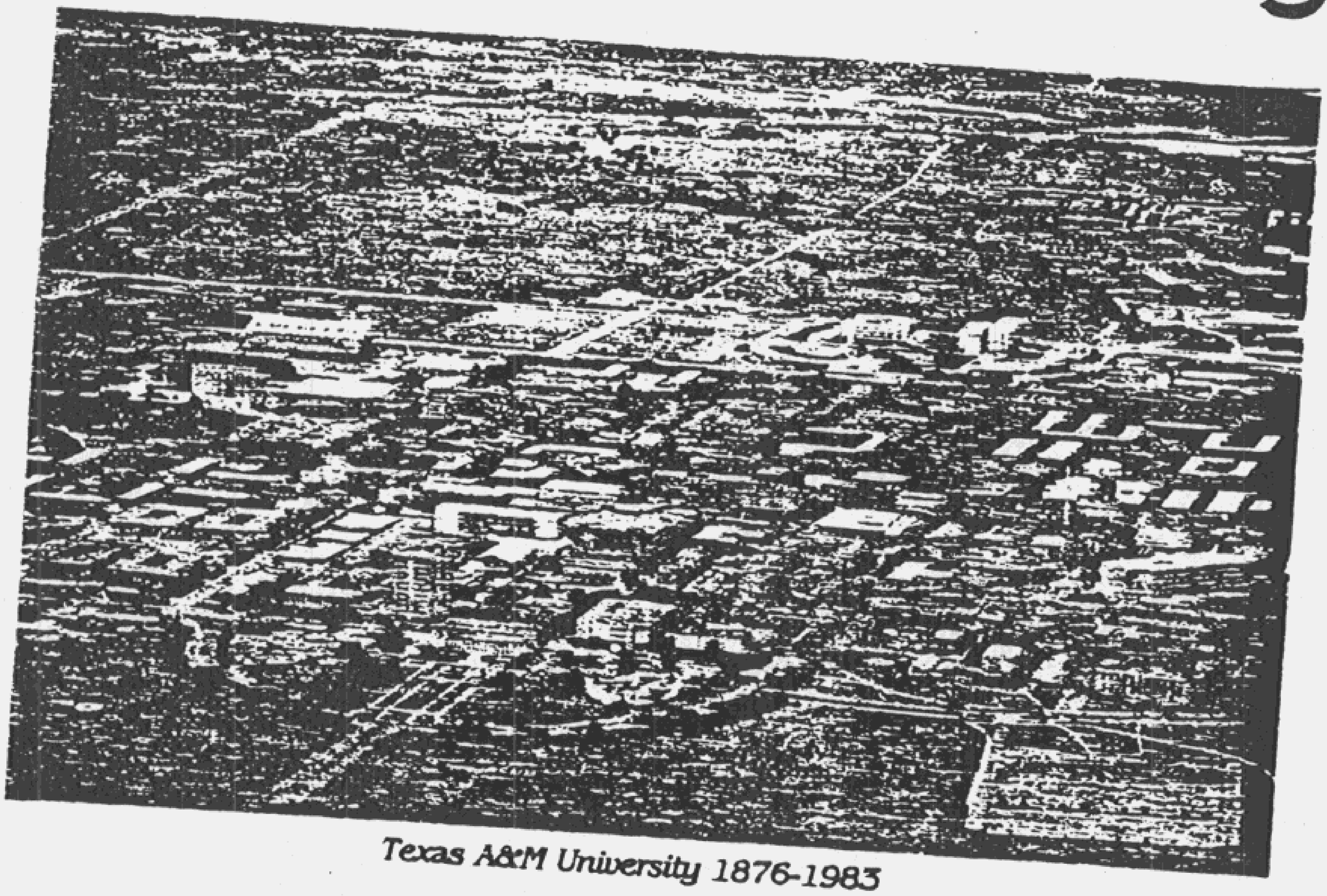

Texas A&M University 1876-1983

UGIM-83

PROCEEDINGS

MAY 25, 26, AND 27, 1983
TEXAS A&M UNIVERSITY
COLLEGE STATION, TEXAS

SPONSORED BY
IEEE COMPONENTS, HYBRIDS AND MANUFACTURING TECHNOLOGY SOCIETY
INTERNATIONAL SOCIETY FOR HYBRID MICROELECTRONICS
IEEE ELECTRON DEVICES SOCIETY

Editor:
Noel R. Strader II

1983 UNIVERSITY/GOVERNMENT/INDUSTRY
MICROELECTRONICS SYMPOSIUM

83CH1906-7

LOW FIELD MOBILITY OF 2-d ELECTRON GAS IN MODULATION DOPED $Al_xGa_{1-x}As$/GaAs LAYERS

K. Lee, M. S. Shur
Department of Electrical Engineering
University of Minnesota
Minneapolis, Minnesota 55455

T. J. Drummond and H. Morkoç
Department of Electrical Engineering and
Coordinated Science Laboratory
University of Illinois
1101 W. Springfield
Urbana, Illinois 61801

Summary

We derive a simple analytical formula for the low field mobility which uses 2-d degenerate statistics for the 2-d electron gas. It also takes into account the finite width of the depletion layer in (Al,Ga)As (which affects primarily impurity scattering), scattering by the charged interface states and polar optical and acoustic phonon scattering. The maximum mobility for a given structure is determined by scattering by the interface charged states. The ultimate mobility which may be achieved is limited by acoustic phonon scattering at about $8\mathrm{x}10^6$ cm^2/Vs for a 2-d electron gas density of $n_{so} \simeq 4\mathrm{x}10^{11}$ cm^{-2}. Our results agree very well with our own and other experimental data.

I. Introduction

In modulation doped structures a two dimensional electron gas is formed at the (Al,Ga)As/GaAs heterointerface due to the electron affinity difference between two materials. The electrons are separated from the donors in the (Al,Ga)As by a thin spacer layer which decreases the impurity scattering and enhances the electron mobility.[1] Screening of the Coulomb potential by the electrons in the inversion layer also enhances the mobility,[2] thus extremely high values of low field mobility have been observed in modulation doped (Al,Ga)As/GaAs structures.[3-5]

In this paper we derive a simple analytical formula for low field mobility. Our approach is an extension of existing theories[6-8] but uses 2-d degenerate statistics for the electron gas. It also takes into account the finite width of the depletion layer in (Al,Ga)As (which affects primarily impurity scattering), scattering by the charged interface states and the polar optical and acoustic phonon scattering.

The mobility limited by the remote donors in the (Al,Ga)As layer is shown to increase with the thickness of the undoped spacer layer, d_i, as $d_i^{5/2}$. The ultimate value of the mobility which may be achieved is limited by the acoustic scattering at about $8\mathrm{x}10^6$ cm^2/Vs for a 2-d electron gas density, $n_{so} \simeq 4.10^{11}$ cm^{-2}. We also show that the maximum experimental mobilities are limited by scattering by charged interface states. Our results agree very well with experimental data obtained in our laboratory as well as other laboratories.[4,5]

II. Scattering Mechanisms

A. Ionized Impurity Scattering Due to Remote Donors

In a modulation doped structure extremely high electron mobility is obtained by separating the free carriers from the donors in (Al,Ga)As (see Fig. 1). The momentum relaxation time $(\tau_{RI})_i$ for electrons in the i-th subband due to the remote donors:[6,9]

$$(1/\tau_{RI})_i = (e^4 mN_d/8\pi\hbar^3\epsilon^2 q)\int_0^{\pi} d\theta\, [\exp(-4qL_i\sin\theta) - \exp(-4qL'_i\sin\theta)]\ \sin\theta/(2q\sin\theta + S_i)^2 \quad (1)$$

Here e is the electronic charge, m is the effective mass, N_d is the remote ionized impurity density assumed to be uniform (see Fig. 1), $\hbar$ is the reduced Plank constant, ϵ is the dielectric permittivity of GaAs, q is the two dimensional electronic wave vector, S_i is the screening constant of the i-th subband (here only intrasubband scattering within the i-th subband is considered) and $L_i = d_i + Z_i$ where d_i is the thickness of the spacer layer and Z_i is the average distance of the electronic wavefunction penetration into GaAs. Equation (1) accounts for the finite width of the depletion layer in the AlGaAs through $L'_i = d_i + Z_i + d_l$ where $d_i + d_l$ is the distance from the heterojunction interface for the boundary between the depletion and neutral region (see Fig. 1). For values of $n_{so} > 10^{11}$ cm^{-2}, the integral in Eq. (1) can be evaluated analytically, because small values of θ determine the integral.

The resulting expression for the momentum relaxation time in the 0-th subband is:

$$(1/\tau_{RI})_o = (e^4 mN_d/64\pi\hbar^3\epsilon^2 q_F^3 S_o^2)\,(1/L_o^2 - 1/L_o'^2) \quad (2)$$

B. Ionized Impurity Scattering Due to Interface Charge States

A two dimensional gas is formed at the GaAs side of an (Al,Ga)As/GaAs heterointerface. Therefore, ther is scattering due to background impurities, the density of which is on the order of 10^{14} cm^{-3}, as well a due to the charged interface states.[10] The corresponding momentum relaxation time, τ_{BI}, is given by:[6]

$$1/\tau_{BI} = (e^4 mN_{BI})/(8\pi\hbar^3\epsilon^2 q_F^2)\cdot I_B(\beta) \quad (3)$$

where N_{BI} is the 2-d impurity density in the potentia well and

$$I_B(\beta) = \int_0^{\pi} d\theta\sin^2\theta/(\sin\theta + \beta)^2 \quad (4)$$

where

$$\beta = S_o/(2q_F) \quad (5)$$

The evaluation of Eq. (3) is very different fro that obtained in references [6,10], because two dimensional degenerate Fermi statistics are used her whereas two[10] dimensional non-degenerate statistics were used previously.

C. Polar Optical Phonon Scattering

An empirical temperature dependent polar optica mobility deduced from bulk GaAs data is used in this work (see Section III).

D. Acoustic Deformation Potential Scattering

We derive the following expressions for the acoustic deformation potential relaxation time:

$$1/\tau_A = e_A^2\, mkT/(\hbar^3\rho_s u^2)\cdot I_A(\gamma) \quad ($$

where

CH1906-7/83/0000-0173 $1.00 © 1983 IEEE

with extremely high mobility observed at low temperature (see Fig. 2). According to our calculations,[14] n_{so} varies as $1/d_i$ when d_i is large ($d_i >> Z_i$). The mobility μ_{RI} limited by the remote donor scattering varies as $n_{so}^{\frac{1}{2}}.d_i^3$ (see Eq. (2) at large values of d_i, i.e. μ_{RI} is proportional to $d_i^{5/2}$. Thus, in theory, a higher value of μ_{RI} can be obtained by increasing the spacer layer thickness. However, the mobility at large d_i is dominated by interface state scattering as shown in Fig. 4. As a result the mobility becomes constant at large values of d_i (see Fig. 3, 4). In other words, the maximum mobility obtained at large d_i is a measure of the interface state density. The values of N necessary to explain the experimental reported in reference 5 and our experimental results are 1.6×10^9 cm^{-2} and 3×10^9 cm^{-2} respectively. Thus, N_{BI} depends on the sample preparation. This may explain why these numbers are less than the value of N_{BI} estimated in reference 15 from the C-V data ($N_{BI} \sim 6 \times 10^{10}$ cm^{-2}).

Also, N_{BI} depends not only on the density of the interface states but also on the position of the Fermi level with respect to the neutral level. This may also contribute to the higher value of N_{BI} measured in reference 15. Some indication of the dependence of N_{BI} on the position of the Fermi level may be inferred from the increase in the low field mobility under illumination. Under illumination the mobility in the sample with d_i = 230 Å[5] was increased from 5.5×10^5 cm^2/Vs to 1.3×10^6 cm^2/Vs. At the same time the value of n_{so} changed from 2.2×10^{11} cm^{-2} to 3.8×10^{11} cm^{-2}. Only part of this mobility increase may be attributed to the increase in screening. Our calculation show that due to the increase in screening the mobility should have increased only to 8×10^5 cm^2/Vs (when the same value of the interface charge N_{BI} is used. We interpret this difference as a result of the decrease in N_{BI} due to the shift in the Fermi level due to the change in n_{so}. According to reference 16.

$$E_F = \Delta E_{FO} + a n_{so} \qquad (21)$$

where $a = 0.125 \times 10^{-12}$ cm^2 eV and $\Delta E_{FO} = 25$ meV at low temperature. (The energy reference in Eq. (21) is the bottom of the conduction band in GaAs at the heterojunction interface. Hence, the change in n_{so} from 2.2×10^{11} cm^{-2} to 3.8×10^{11} cm^{-2} leads to the shift of E_F of the order of $\Delta E_F = 20$ meV. To explain the additional increase of the mobility beyond the increase related to the enhanced screening we have to assume the reduction of N_{BI} to be nearly zero (see Fig. 4). The density of the interface states N_s may be estimated from

$$N_s = \frac{\delta N_{BI}}{\delta E_F} \qquad (22)$$

leading to $N_s = 7.8 \times 10^{10}$ $cm^{-2} eV^{-1}$. This interpretation is also consistent with the general trend exhibited by the experimental curve μ vs. d_i in the range of d_i below 200 Å in Fig. 4. For these values of d_i the value of n_{so} is large enough to shift the Fermi level closer to the neutral level (just as under illumination). Indeed, from the change in measured value of n_{so} and Eq. (21), we estimate the increase in the Fermi level to be roughly 25 meV when d_i is decreased from 300 Å to 150 Å. This should increase the low field mobility over the calculated value because the dependence of N_{BI} on n_{so} is disregarded in our calculation. As can be seen from Fig. 4 this is exactly what is observed experimentally. The temperature dependence of the 2-d electron gas mobility is shown in Fig. 5 where the experimental results agree ve well with the calculated mobility which includes contributions from temperature independent ionize impurity scattering and temperature dependent aco phonon and polar optical phonon scattering. An a rate evaluation of the number of the acoustical phonons is very important at low temperature wher acoustic scattering limits the ultimate value of mobility, being about 8×10^6 cm^2/Vs for $n_{so} = 4 \times 10$ cm^{-2}. This ultimate value of the low field mobil is inversely proportional to n_{so} due to the depen of the Fermi wave vector on n_{so}.

V. Conclusion

We derived simple analytical formulas for the mobility of the 2-d electron gas formed at the (A (Al,Ga)As/GaAs heterointerface. Our theory which takes into account the finite width of the deplet region in the (Al,Ga)As layer, the scattering by t charged interface states and other factor is in a very good agreement with the experimental results.

Acknowledgement

The work at the University of Illinois is fun by the Air Force Office of Scientific Research. Th work at the University of Minnesota is partially funded by the Army Research Office and MEIS Center the University of Minnesota.

Figure Captions

Fig. 1. Energy band diagram of a modulation doped (Al,Ga)As/GaAs heterojunction. Finite thi ness of the ionized (Al,Ga)As layer is sho and the two lowest energy levels in the 2- gas are shown.

Fig. 2. Calculated low field mobility vs. undoped (Al,Ga)As thickness for $n_{so} = 5 \times 10^{11}/cm^2$. Dotted line for $N_d = 0.25 \times 10^{18}/cm^3$, solid line for $N_d = 0.5 \times 10^{18}/cm^3$ and dashed line for $N_d = 1 \times 10^{18}/cm^3$). Dots are experiment points (A from [11], B from [2], C from [1 D from [5] and E from [12], the values for B and C are extrapolated at $n_{so} = 5 \times 10^{11}/cm$

Fig. 3. Experimental mobility vs. undoped (Al,Ga)As thickness. Solid line is from [5] and dash line is from our laboratory [18].

Fig. 4. Comparison between theory and experiment fo the mobility vs. undoped (Al,Ga)As thicknes Two theoretical curves (dotted line for $N_{BI} = 0$ and dashed line for $N_{BI} = 1.5 \times 10^9/cm^2$) are calculated using measured value of 2-d gas density (n_{so}). Experimental values are from [5]. The increase in mobility und illumination is indicated by an arrow.

Fig. 5. Temperature dependence of 2-d gas mobility. Dots are experimental points from ref. [5] and open circles are obtained in our labora tory. Solid line is calculated from Eq. 20 using temperature independent values of $(\mu_{RI}^{-1} + \mu_{BI}^{-1})^{-1} = 2.5 \times 10^6$ cm^2/Vs.

References

[1] T. J. Drummond, H. Morkoç, A. Y. Cho, J. Appl. Phys. 52, 1380 (1981).

[2] H. L. Störmer, A. C. Gossard and W. Wiegmann, Appl. Phys. Lett. 39(6), 493 (1981).

[3] R. Dingle, H. L. Störmer, A. C. Gossard and W. Wiegmann, Appl. Phys. Lett. 33, 665 (1978).

[4] T. J. Drummond, W. Kopp, M. Keever, H. Morkoç and A. Y. Cho, J. Appl. Phys. 53(2), 1023 (1982).

[5] J. V. DiLorenzo, R. Dingle, M. Fever, A. C. Gossard, R. Hendel, J. C. M. Hwang, A. Kastalsky, V. G. Keramidas, R. A. Kiehl and P. O'Connor, IEDM, Tech. Digest 25(1), 578 (1982).

[6] K. Hess, Appl Phys. Lett. 35(7), 484 (1979).

[7] S. Mori and T. Ando, J. of the Phys. Soc. of Japan, 48(3), 865 (1980).

[8] P. J. Price, J. Vac. Sci. Technol., 19(3), 599 (1981).

[9] Y. Takeda, H. Kamei and A. Sasaki, Electronics Lett. 18(7), 310 (1982).

[10] C. T. Sah, T. H. Ning and L. L. Tschopp, Surf. Sci. 32, 561 (1972).

[11] T. J. Drummond, H. Morkoç, K. Hess and A. Y. Cho, J. Appl. Phys. 52, 5231 (1981).

[12] S. Hiyamizu, T. Fujii, T. Mimura, K. Nanbu, J. Saito and H. Hashimoto, Jap. J. of Appl. Phys. 20(6), L455 (1981)

[13] D. L. Rode, Phys. Rev. B, 2(4), 1012 (1970).

[14] K. Lee, M. S. Shur, T. J. Drummond and H. Morkoç, J. Appl. Phys., unpublished.

[15] H. Kroemer, Wu-Yi Chien, J. S. Harris, Jr. and D. D. Edwall, Appl. Phys. Lett. 36(4), 295 (1980).

[16] T. J. Drummond, H. Morkoç, K. Lee and M. Shur, IEEE Elect. Dev. Lett. EDL-3, 338 (1982).

[17] D. C. Tsui, a. C. Gossard, G. Kaminsky and W. Wiegmann, Appl. Phys. Lett. 39(9), 712 (1981).

[18] J. Klem, T. Masselink, D. Arnold, R. Fischer, T. J. Drummond, H. Morkoç, K. Lee and M. Shur, unpublished.

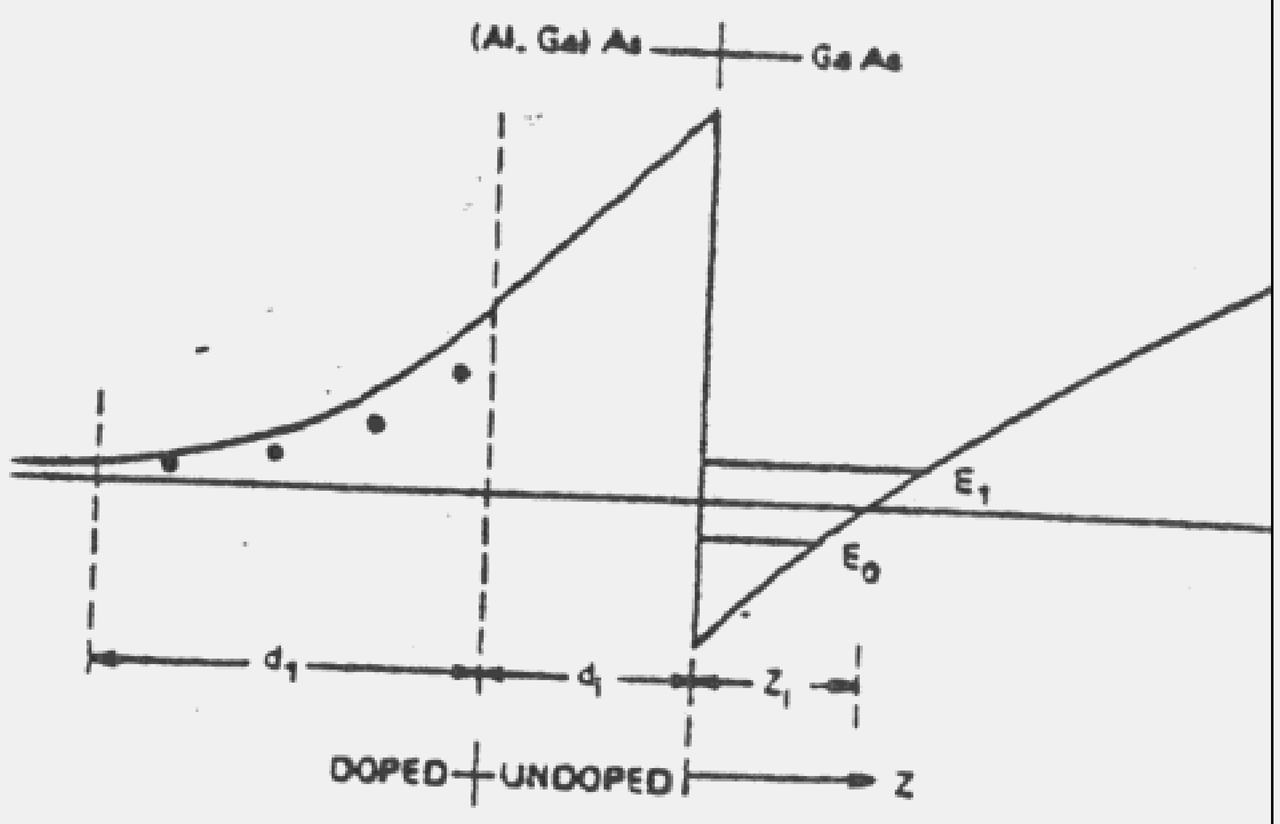

Figure 1

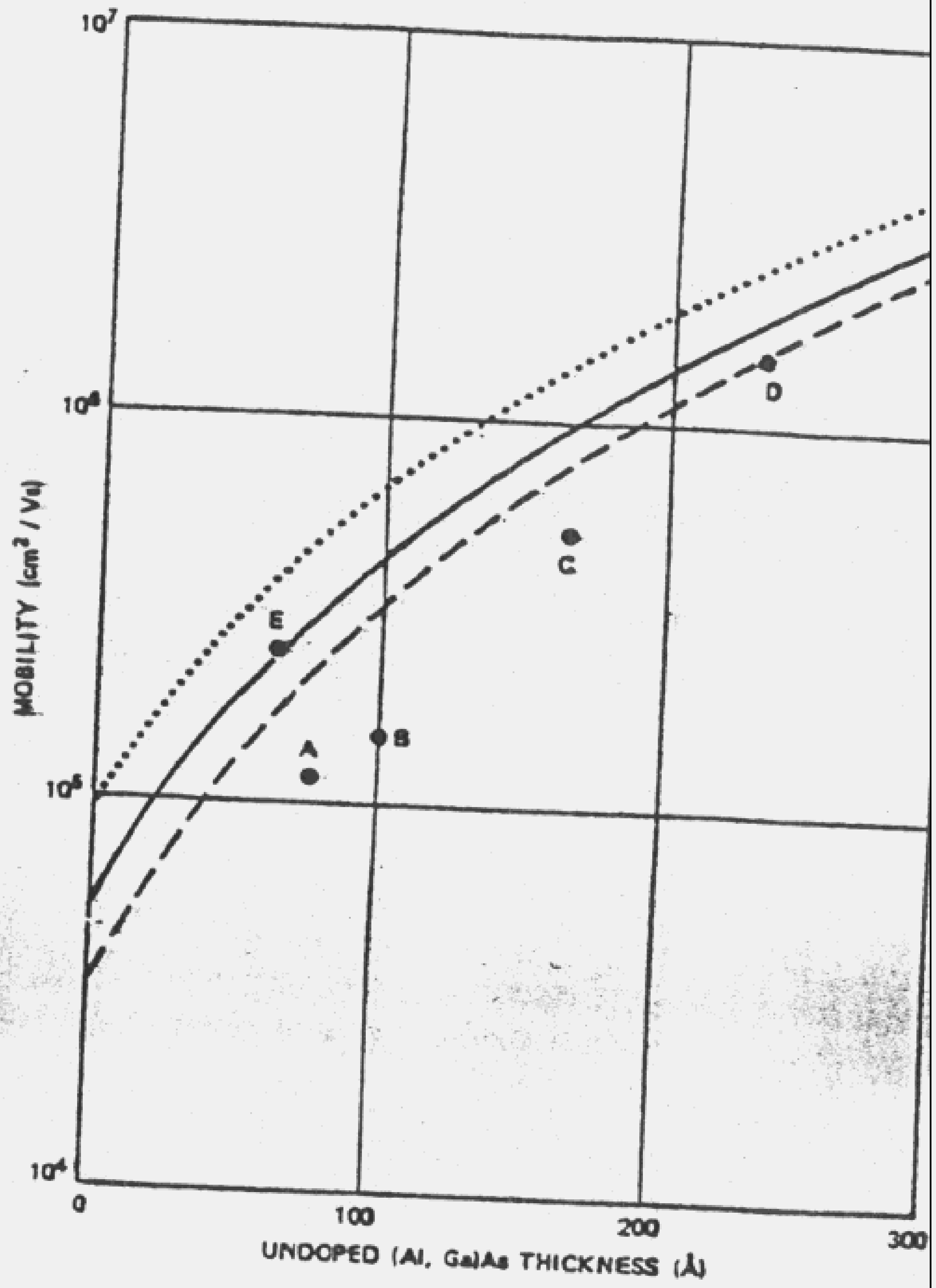

Figure 2

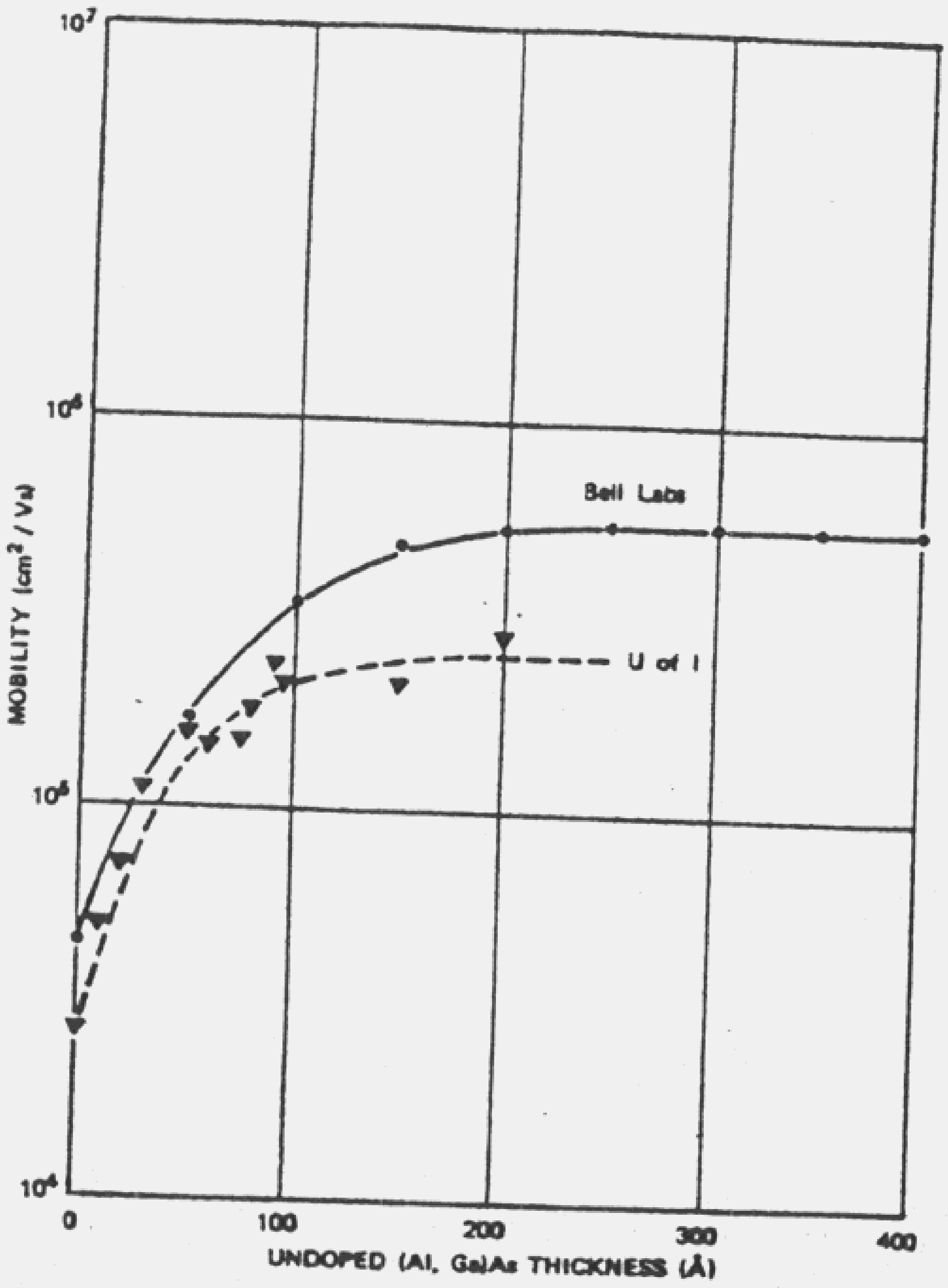

Figure 3

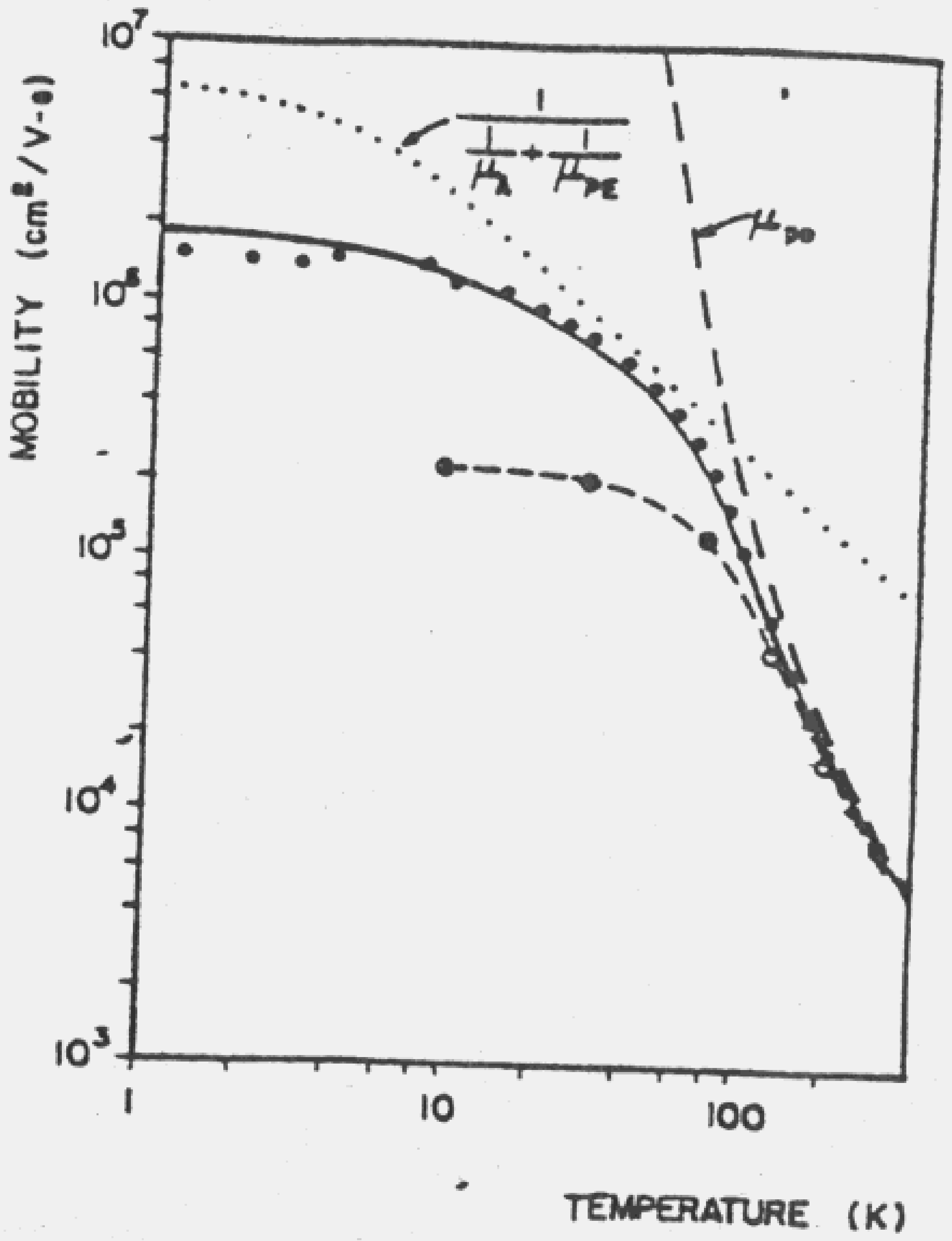

Figure 5

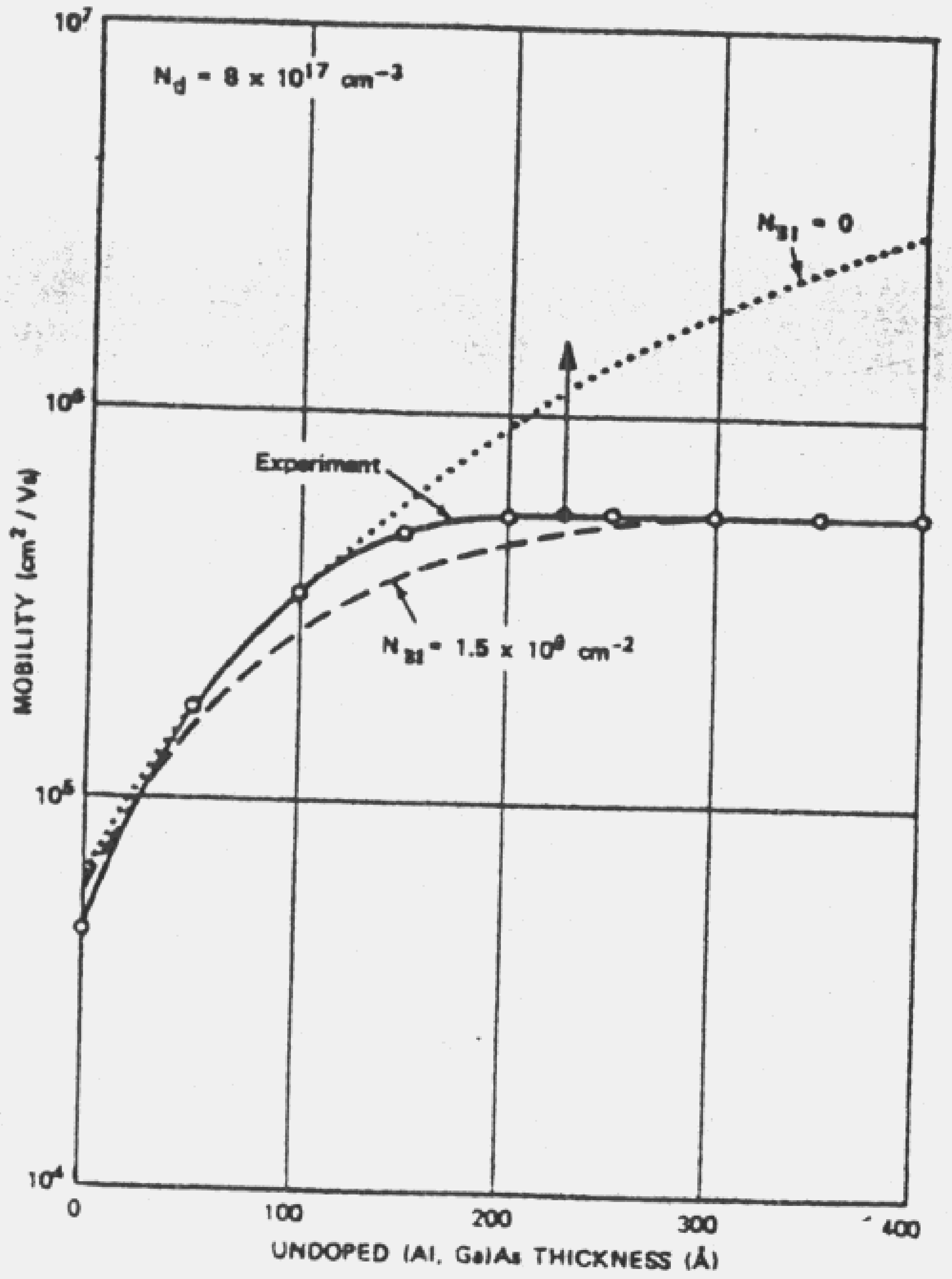

Figure 4